Supplementary Figure 1

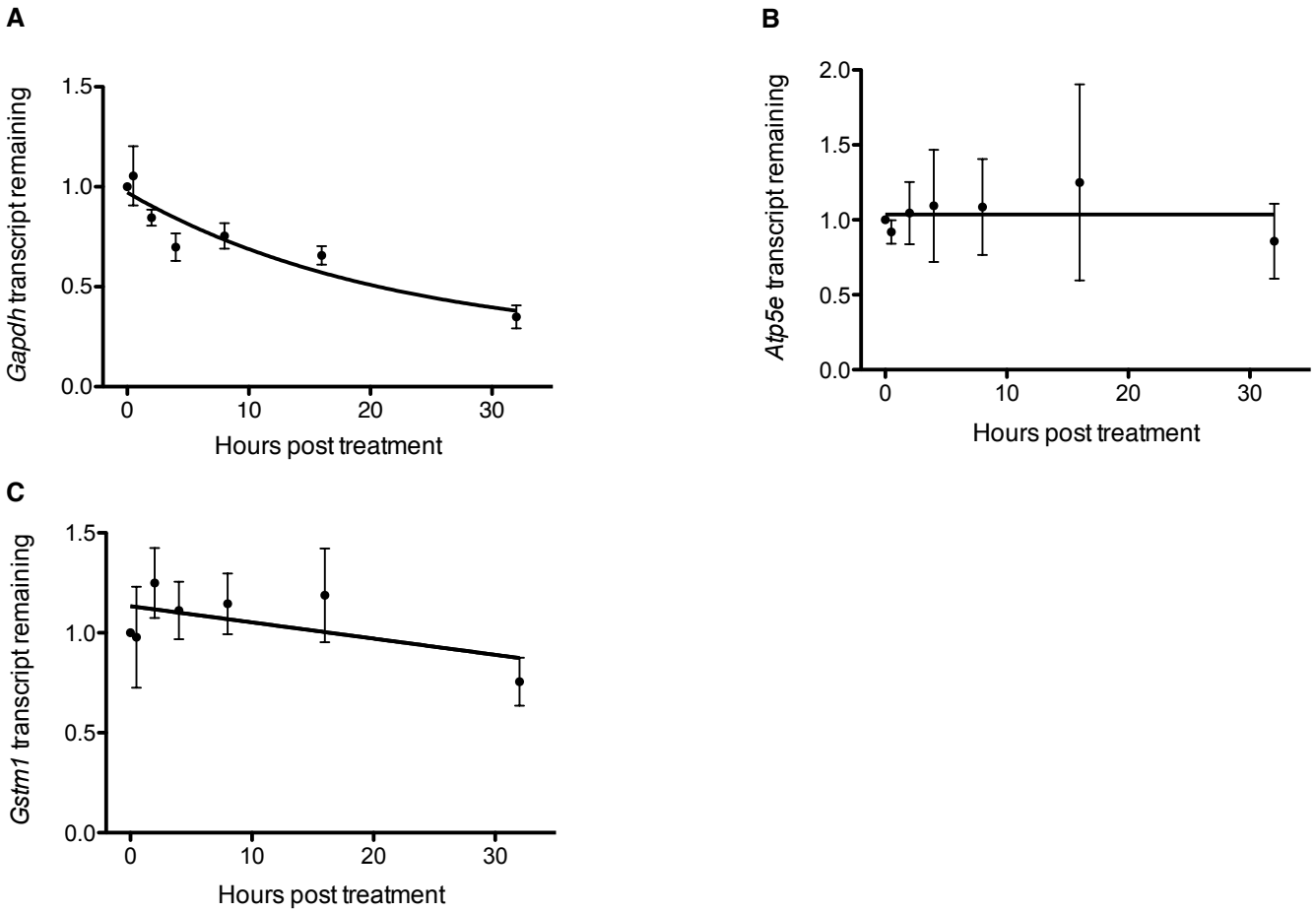

Figure S1A: *Gapdh* is not stable over a 32 hour time-course
Transcript decay curve for *Gapdh* in N2A cells after blocking transcription with Actinomycin D and measuring transcript remaining relative to *Atp5e* by qPCR. Two biological replicates. Half-life of 15 h 2 min determined by one phase decay using non-linear regression. R2 = 0.92.

Fig S1B: Transcript decay curve for *Atp5e.*
Transcript decay curve N2A cells after blocking transcription with Actinomycin D and measuring transcript remaining relative to *Zfas1* by qPCR. *Atp5e* and *Zfas*1 stability is very similar. Three biological replicates. Error bars are standard deviations. Non-linear regression was performed to compare linear decay vs straight line using the Akaike information criterion (AICc). Straight line is preferred. Confirmed by F-test from linear regression, which showed no significant deviation of slope from zero.

Fig S1C: Transcript decay curve for *Gstm1*
Transcript decay curve in N2A cells after blocking transcription with Actinomycin D and measuring transcript remaining relative to *Zfas1* by qPCR. Three biological replicates. Error bars are standard deviations. Non-linear regression was performed to compare linear decay vs straight line using the AICc. Linear decay is preferred. However, an F-test from linear regression shows no significant deviation of the slope from zero.

Supplementary Figure 2

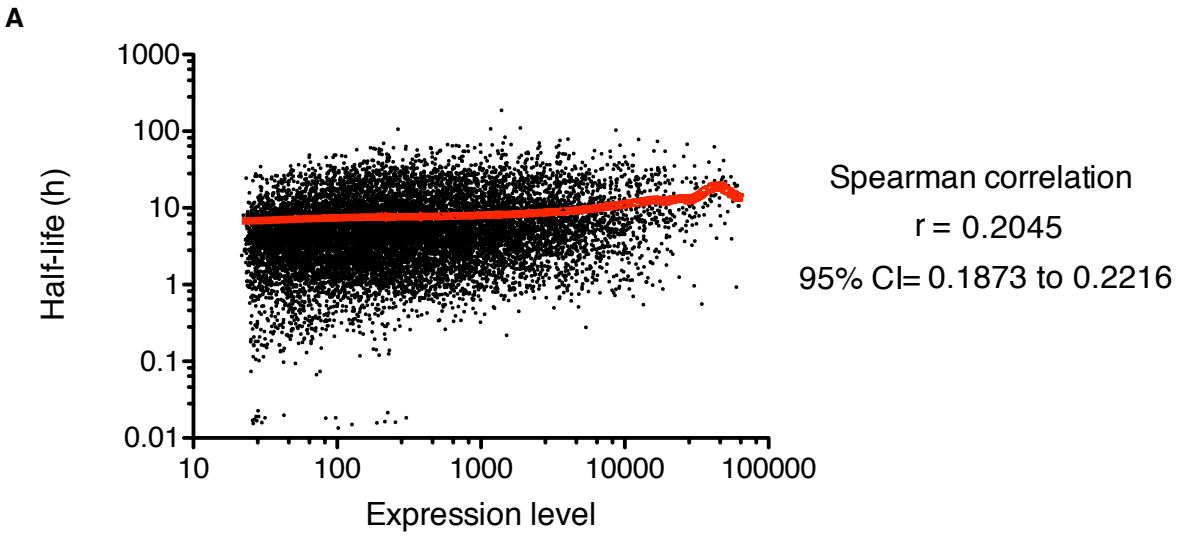

Figure S2A: Correlation between expression level and half-life.
Half-life values were calculated by one phase decay or linear decay. Expression values are estimated Y0 values from one phase decay curve fitting or intercept values from linear decay. Axes are log 10. Coarse Lowess curve is shown in red. A small positive correlation between expression and half-life (Spearman correlation P <0.0001) is observed. Spearman correlation was calculated as data is not gaussian. Results show no sign of a trend to longer half-lives for lowly expressed transcripts near the expression cutoff (which could have suggested the expression cuttoff was too low and affected by background).

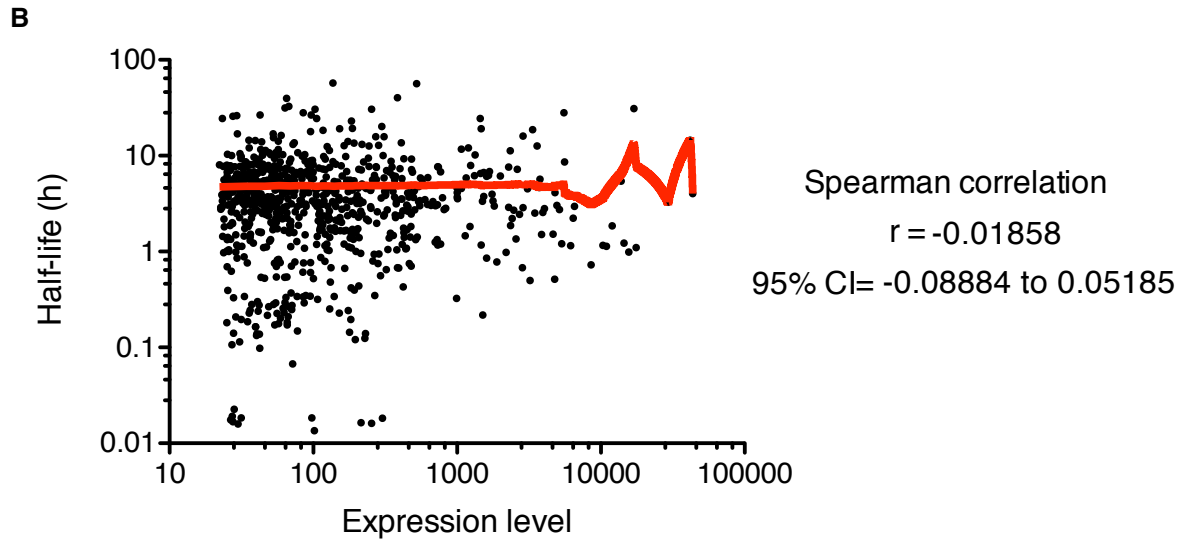

Figure S2B: Correlation between expression level and half-life of lncRNAs.
Half-life values were calculated by one phase decay or linear decay. Expression values are estimated Y0 values from one phase decay curve fitting or intercept values from linear decay. Axes are log 10. Coarse Lowess curve is shown in red. There is no correlation between expression and half-life (Spearman correlation P= 0.5945). Spearman correlation was calculated as data is not gaussian. Results show no sign of a trend to longer half-lives for lowly expressed transcripts near the expression cutoff (which could have suggested the expression cuttoff was too low and affected by array background).

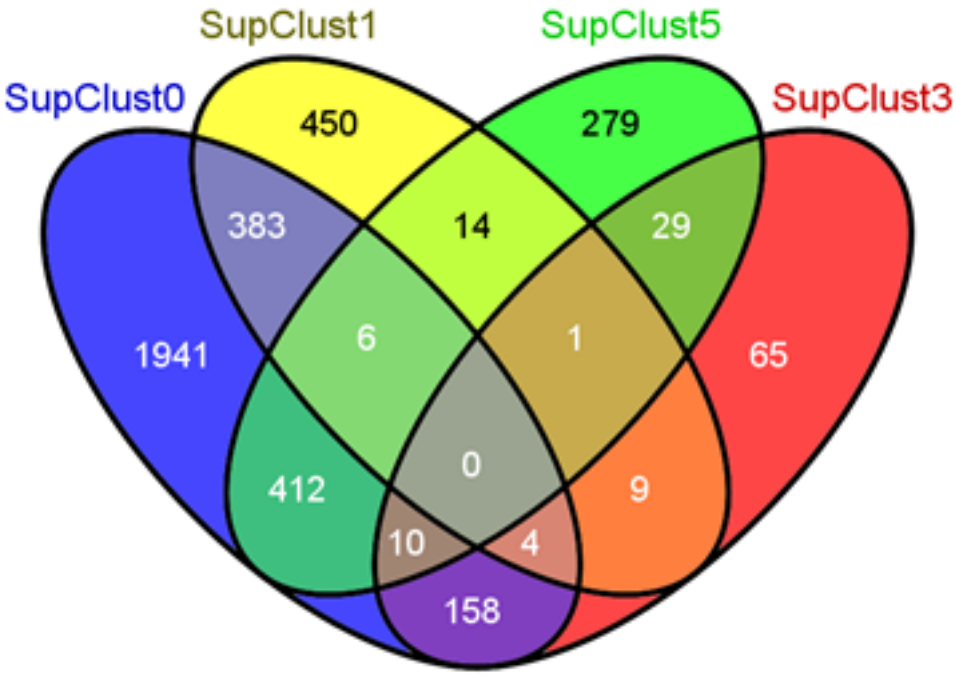

Figure S3: Identification of genes with multiple probes that cluster in different super-clusters
Unigene genes present in any of the four most populous super-clusters were filtered for those containing two or more probes. Venn diagram of probe overlap made using Venny (bioinfogp.cnb.csic.es/tools/venny/). Numbers show number of Unigene genes where all probes are found in one super-cluster or in multiple super-clusters.

Supplementary Figure 4

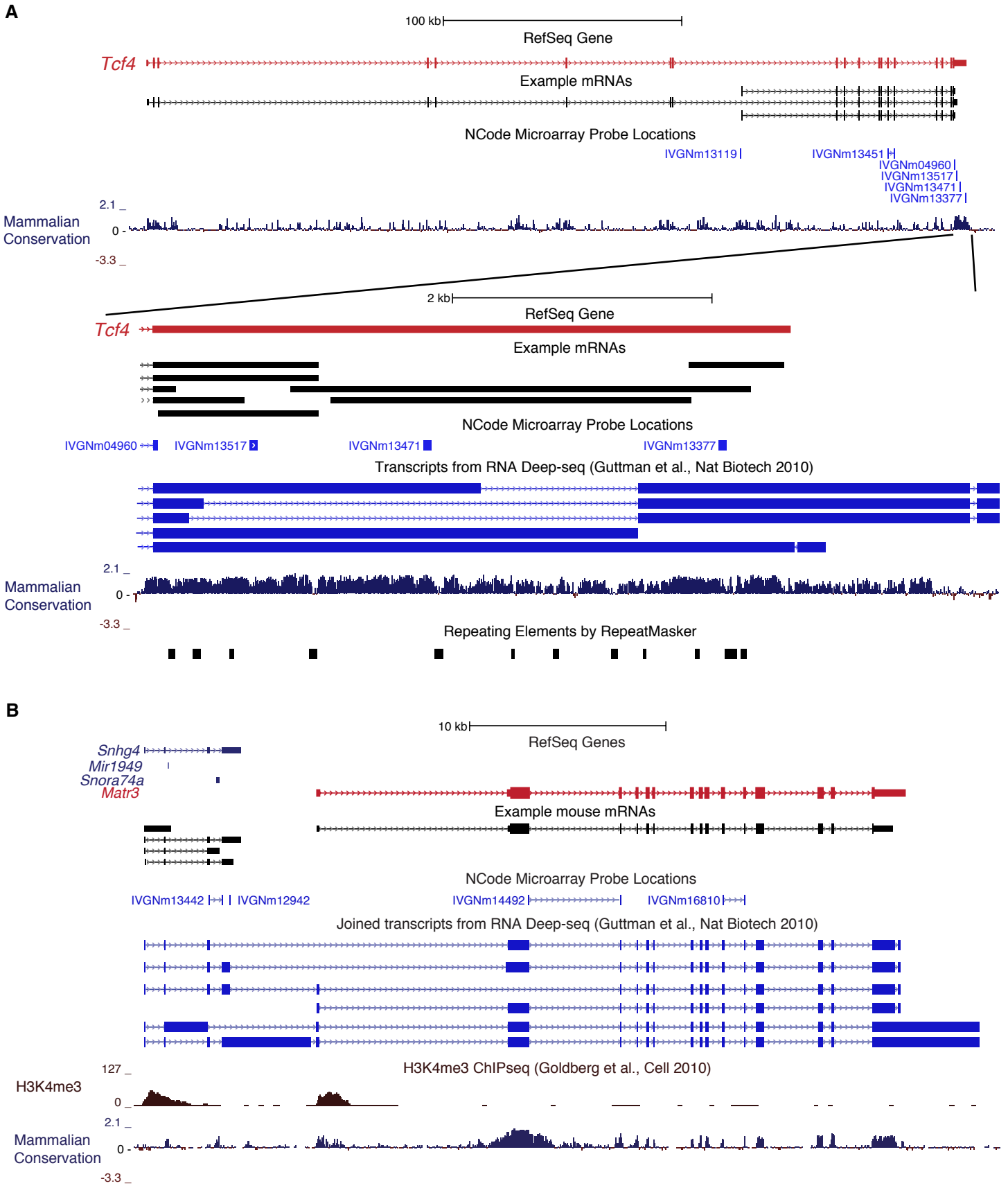

Figure S4: Genomic context of transcripts of interest. Figure shows refseq gene(s), representative examples of both known mRNAs and transcripts constructed from deep-sequencing of RNA (Guttman et al. 2010). Introns – thin, arrowed lines. Exons - boxes. Also shown are positions of Ncode microarray probes used to determine transcript half-lives. A) *Tcf4* gene locus and blow-up of the 3'UTR region. Probes: IVGNm1345 and IVGNm04960 are to universal *Tcf4* splice junctions, IVGNm13517, IVGNm13471 and IVGNm13377 to the 3'UTR, IVGNm13119 is to an intronic mRNA that may be part of the shorter*Tcf4* isoform. B) *Snhg4-Matr3* genomic locus. Positions of known transcriptional start sites shown by HeK4me3 (Goldberg et al. 2010).

Goldberg AD, Banaszynski LA, Noh KM, Lewis PW, Elsaesser SJ, Stadler S, Dewell S, Law M, Guo X, Li X et al. 2010. Distinct factors control histone variant H3.3 localization at specific genomic regions. *Cell* **140**: 678-691.

Guttman M, Garber M, Levin JZ, Donaghey J, Robinson J, Adiconis X, Fan L, Koziol MJ, Gnirke A, Nusbaum C et al. 2010. Ab initio reconstruction of cell type-specific transcriptomes in mouse reveals the conserved multi-exonic structure of lincRNAs. *Nat Biotechnol* **28**: 503-510.

Supplementary Figure 5

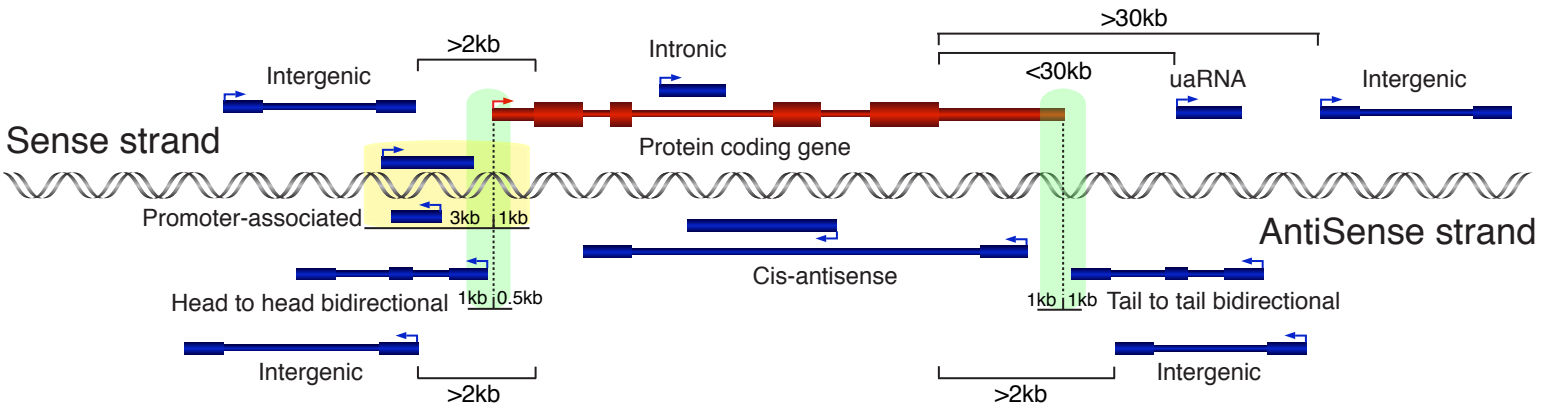

Figure S5: Classification of lncRNAs by genomic context.

Figure shows different classifications of lncRNAs based on their genomic context. Classifications are based on locations of lncRNAs compared to known coding genes. Hypothetical protein coding gene shown in red. LncRNAs in blue. Arrows show direction of transcription. Thick boxes represent coding exons, medium boxes are noncoding exons, while thin boxes are introns. Green shaded area at 5' of coding gene represents region in which a lncRNA on the opposite strand can initiate and be classified as head to head bidirectional. Green shaded area at 3' of coding gene represents region in which a lncRNA can terminate and be classified as tail to tail bidirectional. Yellow shaded area represents region in which a lncRNA can initiate and terminate and be classified as promoter-associated. Note that aside from promoter-associated lncRNAs classifications were not affected by the presence of absence of introns in the lncRNAs. Image not to scale.

Full definitions:

Intergenic transcripts were defined as ncRNAs not transcribed within 2kb upstream of a protein-coding region on either strand or 30 kb downstream in sense direction or 2kb downstream in antisense direction.

3'UTR-associated transcripts (uaRNAs) were defined as as any ncRNA that initiates within 30 kb downstream of a stop codon on the same strand (to allow for the potential of 3'UTRs that extend beyond their annotations (Moucadel et al. 2007; Mercer et al. 2011)).

Head to head transcripts from bidirectional promoters were defined as transcripts that originate from the antisense strand within 1 kb upstream or 0.5 kb downstream of the 5' end of another RNA transcriptional start site.

Tail to tail transcripts terminate on the antisense strand within 1000 nt downstream or 1000 nt overlapping the termination site of another transcript.

Cis-antisense transcripts were defined as those lncRNAs where at least 90% of their exonic length overlapped with a transcript on the opposite strand.

Exclusively intronic ncRNAs were defined as those that initiated and terminated within introns of protein-coding genes in the sense orientation.

Inclusive intronic ncRNAs included any sense noncoding transcript where at least 75% of its exonic region covers the introns of a protein-coding gene and allowed transcript initiation and/or termination within the coding gene exons.

Promoter-associated transcripts were defined as single exon transcripts whose transcription was found within 3kb upstream and 1kb downstream of transcription start sites on either strand.

Note 1: Some lncRNA genomic categories are mutually exclusive but others are not.

Note 2: Some lncRNA genomic categories are defined by the distance from a protein coding gene (intergenic, uaRNA, intronic) while others use the distance from any known transcript (bidirectional, cis-antisense, promoter-associated)

Mercer TR, Wilhelm D, Dinger ME, Solda G, Korbie DJ, Glazov EA, Truong V, Schwenke M, Simons C, Matthaei KI et al. 2011. Expression of distinct RNAs from 3' untranslated regions. Nucleic Acids Res 39: 2393-2403.

Moucadel V, Lopez F, Ara T, Benech P, Gautheret D. 2007. Beyond the 3' end: experimental validation of extended transcript isoforms. Nucleic Acids Res 35: 1947-1957.

Supplementary Figure 6

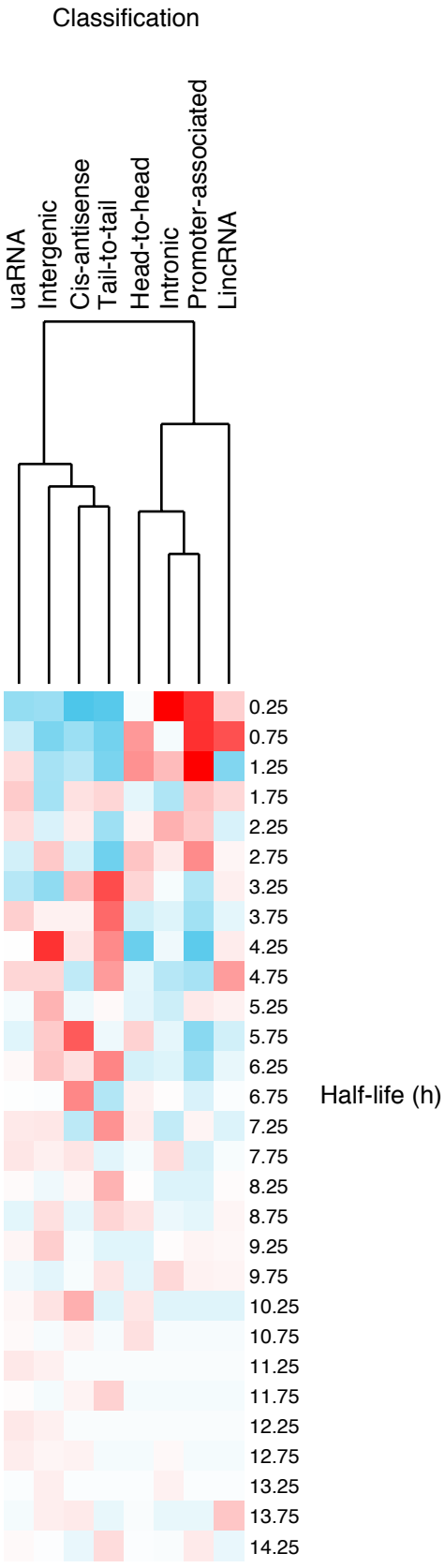

Figure S6: Unsupervised hierarchical clustering of lncRNA classes defined by genomic location.

A frequency distribution for each class was created by calculating the proportion of transcript half-lives found in half-hour bins. Time-points record the centre of each bin. Clustering was performed using cluster3 (de Hoon et al. 2004), and visualized in Java Treeview (Saldanha 2004). Each row/time-point was centered by subtracting the mean proportion. Blue values – proportion below mean. Red values – proportion above mean. Clustering was performed on all bins between 0 and 14.5 h (the last time point 1% of transcripts were present for 2 or more genomic classifications).

de Hoon MJ, Imoto S, Nolan J, Miyano S. 2004. Open source clustering software. *Bioinformatics* 20: 1453-1454.

Saldanha AJ. 2004. Java Treeview--extensible visualization of microarray data. *Bioinformatics* 20: 3246-3248.

Supplementary Figure 7

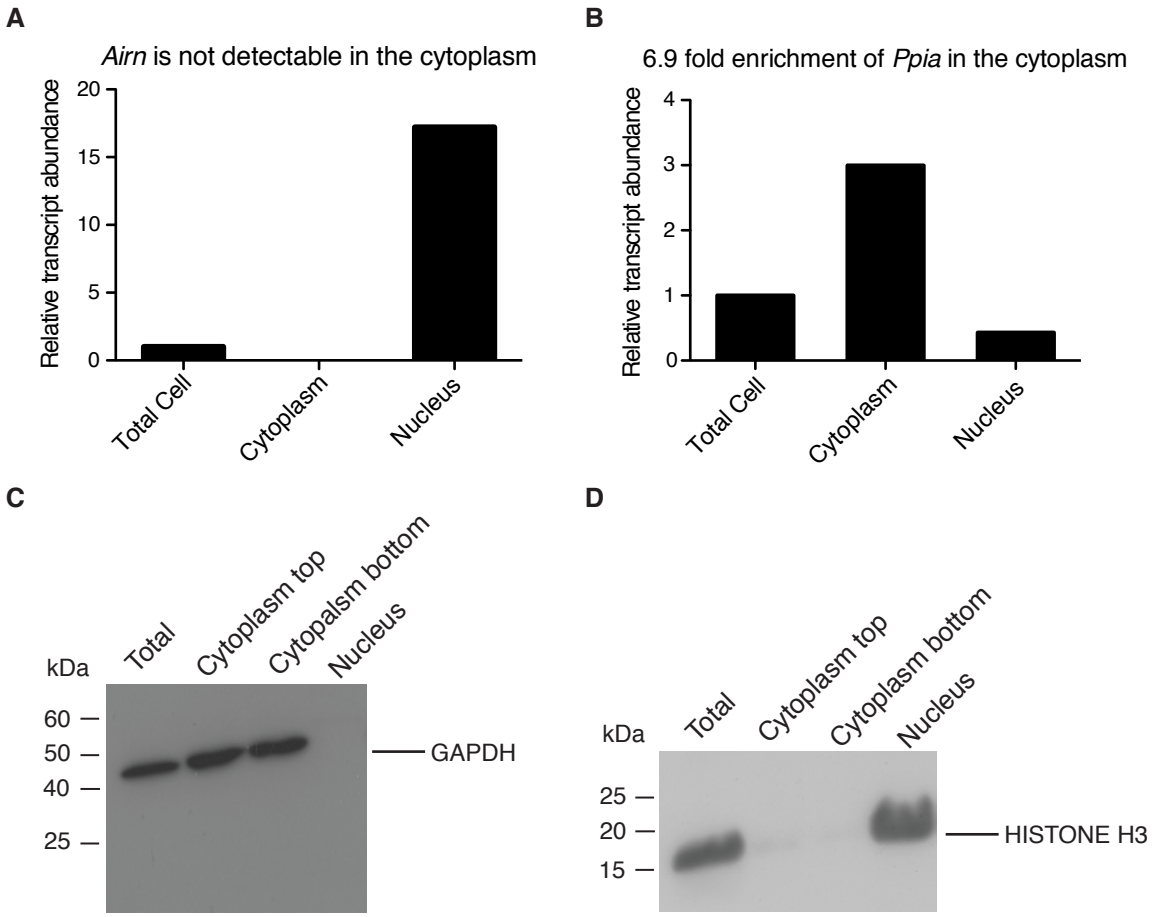

Figure S7: Confirmation of fraction purity in N2A cells
A & B: Results of qPCR using the nuclear marker *Airn* (A) and the cytoplasmic marker *Ppia* (B). Results show relative enrichment of each transcript in the nucleus and cytoplasm (per cell) in a representative fractionation. The expression level in whole cells (sample taken before fractionation) served as a baseline to measure relative enrichment against. C & D: Western analysis of cell fractionation. C: Detection of GAPDH specifically in cytoplasm and total cell. D: Detection of HISTONE H3 in nuclei and whole cells. Top and bottom of cytoplasmic supernatant were collected separately and the purity of both was tested.

Supplementary Figure 8

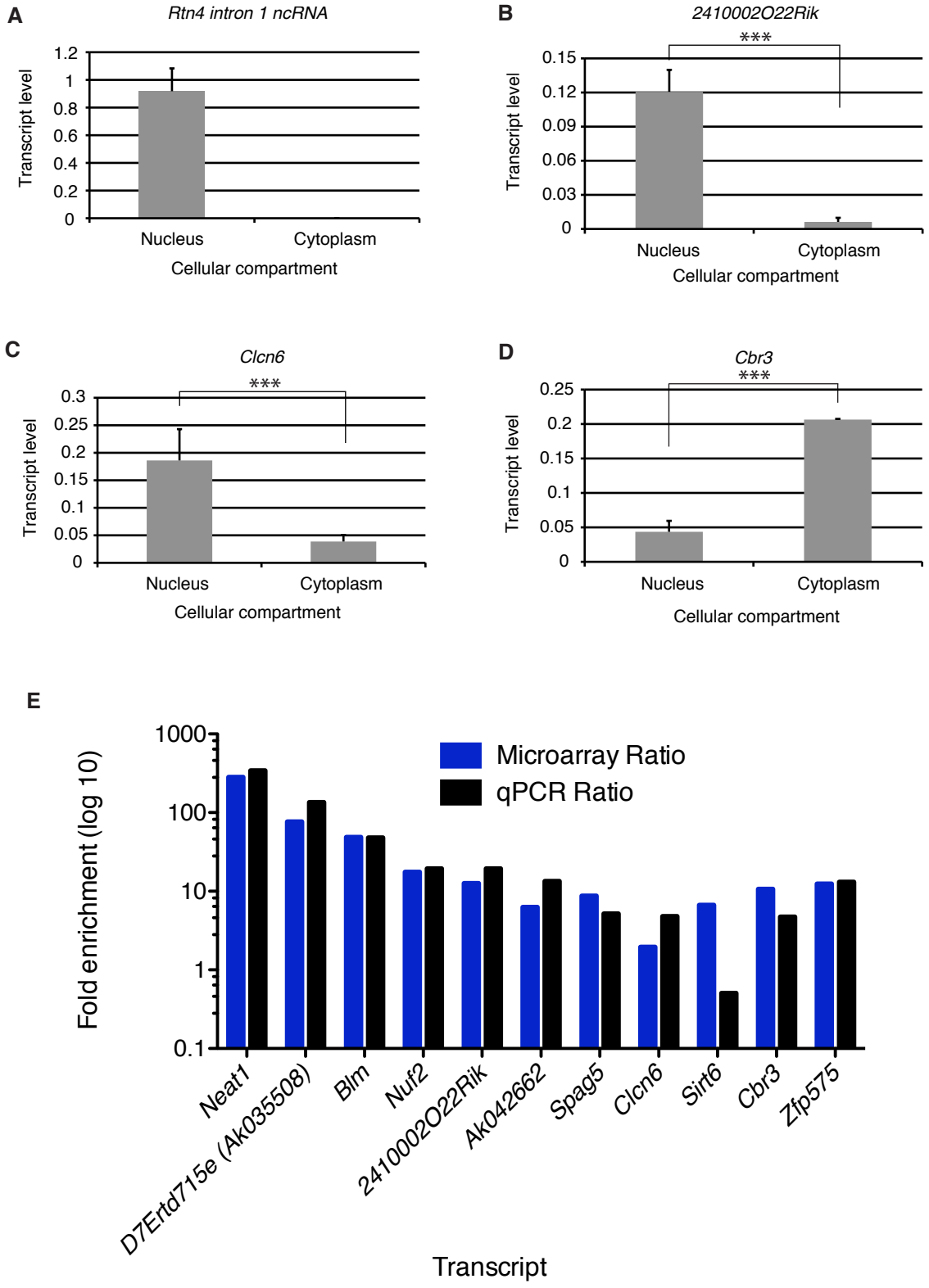

Figure S8: qPCR validation of differentially expressed transcripts
A-D: Examples of qPCR analysis, investigating the expression levels of transcripts identified by microarray as differentially localized between the nucleus and cytoplasm. Transcript levels were determined by absolute quantification of three biological replicates. *** P <0.0001. Note: Expression levels are not comparable between different transcripts. E: Comparison of the nuclear/cytoplasmic enrichments determined by qPCR to those determined by microarray. Included are nuclear and cytoplasmically enriched transcripts. Note: *Rtn4 intron 1* ncRNA is not present in panel E as it appears to be entirely nuclear specific and hence a ratio could not be calculated.

Supplementary Figure 9

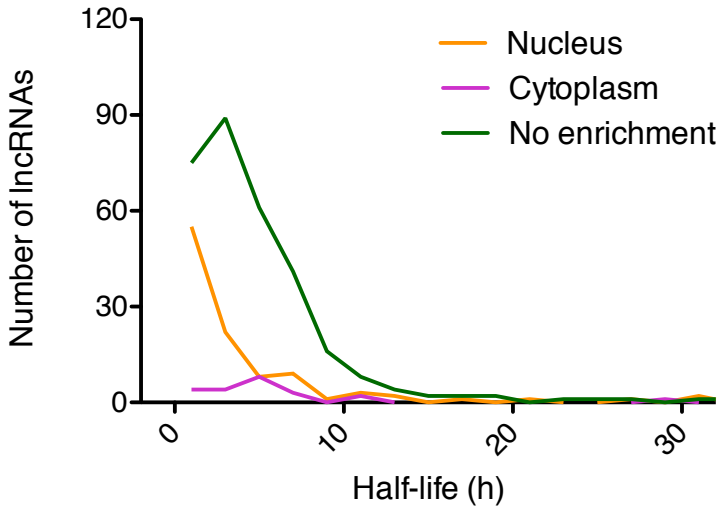

Figure S9: Half-lives of all localized lncRNAs
Frequency distribution showing the number of nuclear and cytoplasmically enriched plus non-enriched lncRNAs transcripts. Transcripts divided into 2 h half-life bins. Plotted points are at the centre of the 2 h bin. Only time-points with 1% or more of transcripts are plotted.

Supplementary Figure 10

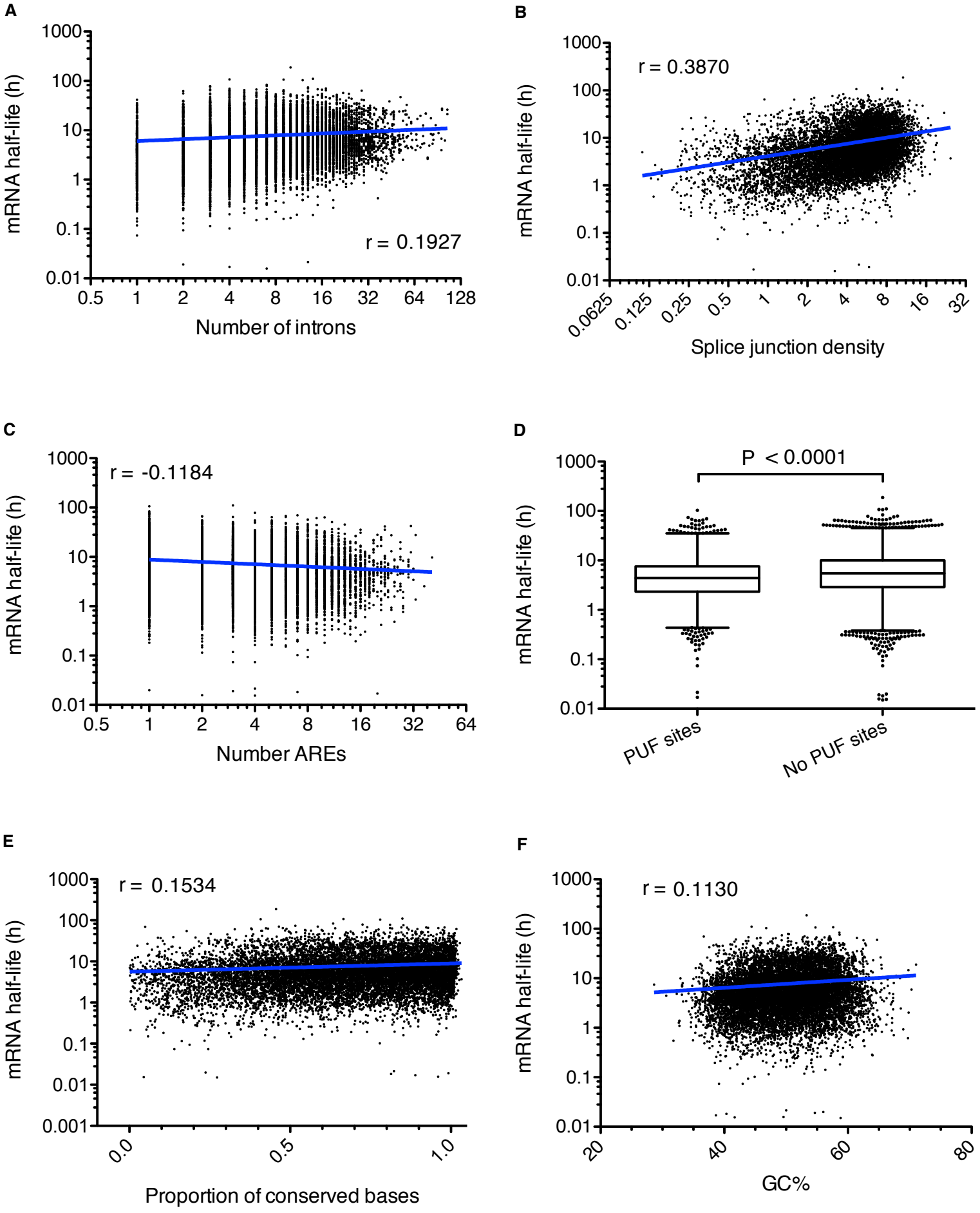

Figure S10: Relationship between stability and mRNA transcript features

A) Positive correlation between mRNA half-life and intron number in spliced transcripts.
Significant relationship between mRNA transcripts with a greater number of introns and increased stability. Spearman correlation = 0.1927 ($P < 0.0001$). 95% CI = 0.1744 to 0.2109. Trend line shows a log-log fit from nonlinear regression. Axes are log10-log 2.
B) Positive correlation between mRNA half-life and splice junction density in spliced transcripts. Significant relationship between mRNA transcripts with a greater density of splice junctions (junctions per kb transcript) and increased stability. Spearman correlation = 0.3870 ($P < 0.0001$). 95% CI = 0.3708 to 0.4030. Trend line shows a log-log fit from nonlinear regression. Axes are log10-log 2
C) Increasing numbers of AU rich elements correlate with lower mRNA half-lives
Significant negative correlation between number of AREs (calculated across the entire mRNA transcript) compared to mRNA half-life. Spearman correlation = -0.1184. $P < 0.0001$. 95% CI = -0.1386 to -0.09824. Counting AREs in 3'UTRs only gave a weaker but still significant Spearman correlation = -0.06050. $P < 0.0001$. Increased strength of correlation over whole transcripts suggests effect of AREs are not limited to 3'UTRs and so should be detectable in lncRNAs (which do not have 3'UTRs). Trend line shows a log-log fit from nonlinear regression. Log10-log2 plot.
D) Comparison of the stability of mRNAs with and without PUF protein binding motifs
Box and whisker plot of mRNA half-lives. Whiskers show 1-99th percentile, with individual transcripts outside this shown as dots. Box represents the 25-75th percentile. Difference calculated using a nonparametric Mann-Whitney t-test ($P < 0.0001$). Demonstrates that mRNA transcripts containing one or more PUF binding site (found anywhere within the mRNA transcript) are less stable than those without.
E) Positive correlation between mRNA conservation and half-life
Spearman correlation between conservation (proportion of transcript bases that overlap PhastCons elements) and half-life = 0.1534 ($P < 0.0001$). 95% CI = 0.1353 to 0.1715. Significant relationship between transcripts with a greater proportion of conserved bases and increased stability. Trend line shows a semilog fit from nonlinear regression. Log10-linear plot.
F) Positive correlation between mRNA GC% and half-life
Spearman correlation between GC% and half-life of mRNAs = 0.1130 ($P < 0.0001$). 95% CI = 0.09460 to 0.1312. Significant relationship between transcripts with a higher GC% and increased stability. Trend line shows a semilog fit from nonlinear regression. Log10-linear plot.

Supplementary Figure 11

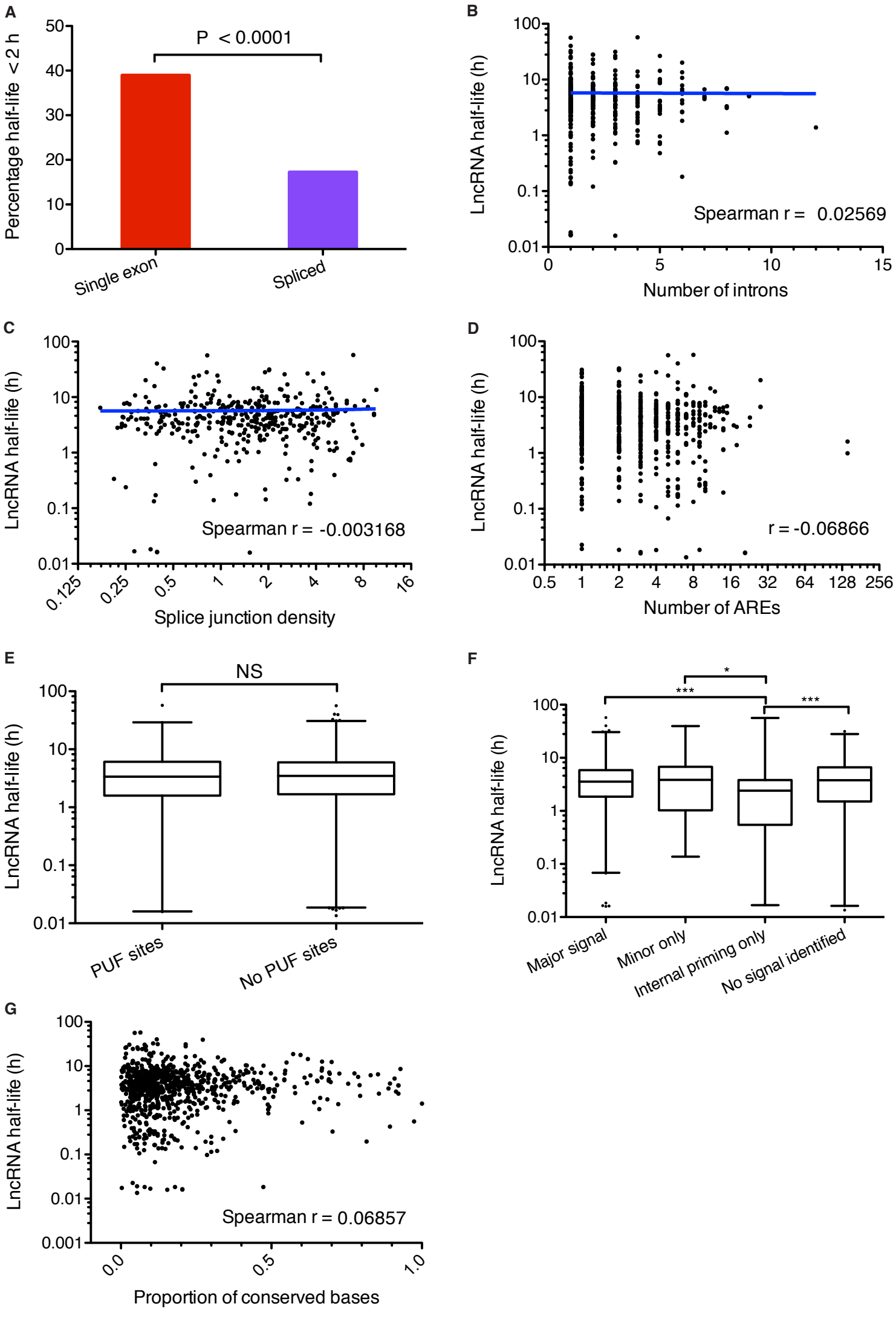

Figure S11: Relationship between stability and lncRNA transcript features

A) Overrepresentation of single exon lncRNAs amongst unstable transcripts
Percentage of unstable (half-life under 2 h) single exon versus spliced lncRNA transcripts. Significant difference calculated using Fisher's exact test.
B) No correlation between half-life of spliced lncRNAs and intron number
Testing for any relationship between the half-life of spliced lncRNAs and the number of introns. Spearman correlation = 0.02569. Not significant. 95% CI = -0.07688 to 0.1277. Linear regression is shown in blue. Slope of linear regression is not significantly different from zero (P = 0.9322). Log10-linear plot.
C) No correlation between half-life of spliced lncRNAs and splice junction density
Testing for any relationship between half-life of spliced lncRNAs and the density of splice junctions (number of junctions per kb of mature transcript). Spearman correlation = -0.003168. Not significant. 95% CI = -0.1055 to 0.09924. Linear regression is shown in blue. Slope of linear regression is not significantly different from zero (P = 0.7622). Log10-log2 plot.
D) Relationship between the number of AU rich elements (AREs) and lncRNA half-lives
No significant correlation between lncRNAs with AREs (1 or more) and lncRNA half-lives. Spearman correlation = -0.06866, Not significant: P = 0.0907. 95% CI = -0.1497 to 0.01329. Closeness to statistical significance at 95% level suggests negative correlation could be significant with large samples sizes. Log10-log2 plot.
E) Comparison of the stability of lncRNAs with and without PUF protein binding motifs.
Box and whisker plot of lncRNA transcript half-lives. Whiskers show 1-99th percentile, with individual transcripts outside this shown as dots. Box represents the 25-75th percentile. Difference calculated using a nonparametric Mann-Whitney t-test (P = 0.308). Y axis is log10.
F) Comparison of stability of lncRNAs with and without identified polyadenylation signals
Box and whisker plot. Whiskers show 1-99th percentile, with individual transcripts outside this shown as dots. Box represents the 25-75th percentile. Differences between groups calculated with a 1way ANOVA with Kruskal-Wallis non-parametric test and Dunn's post test to compare individual annotations. * $P < 0.05$, *** $P < 0.001$.
G) Correlation between lncRNA transcript conservation and half-life.
Spearman correlation = 0.06857. P = 0.0498. 95% CI = -0.001978 to 0.1384. Indicates a small positive relationship between increased half-life and lncRNAs with higher conservation. Spearman correlation utilized because neither half-life data nor conservation data is Gaussian. Conservation is proportion of transcript bases overlapping PhastCons elements. Log10-linear plot.

Supplementary Figure 12

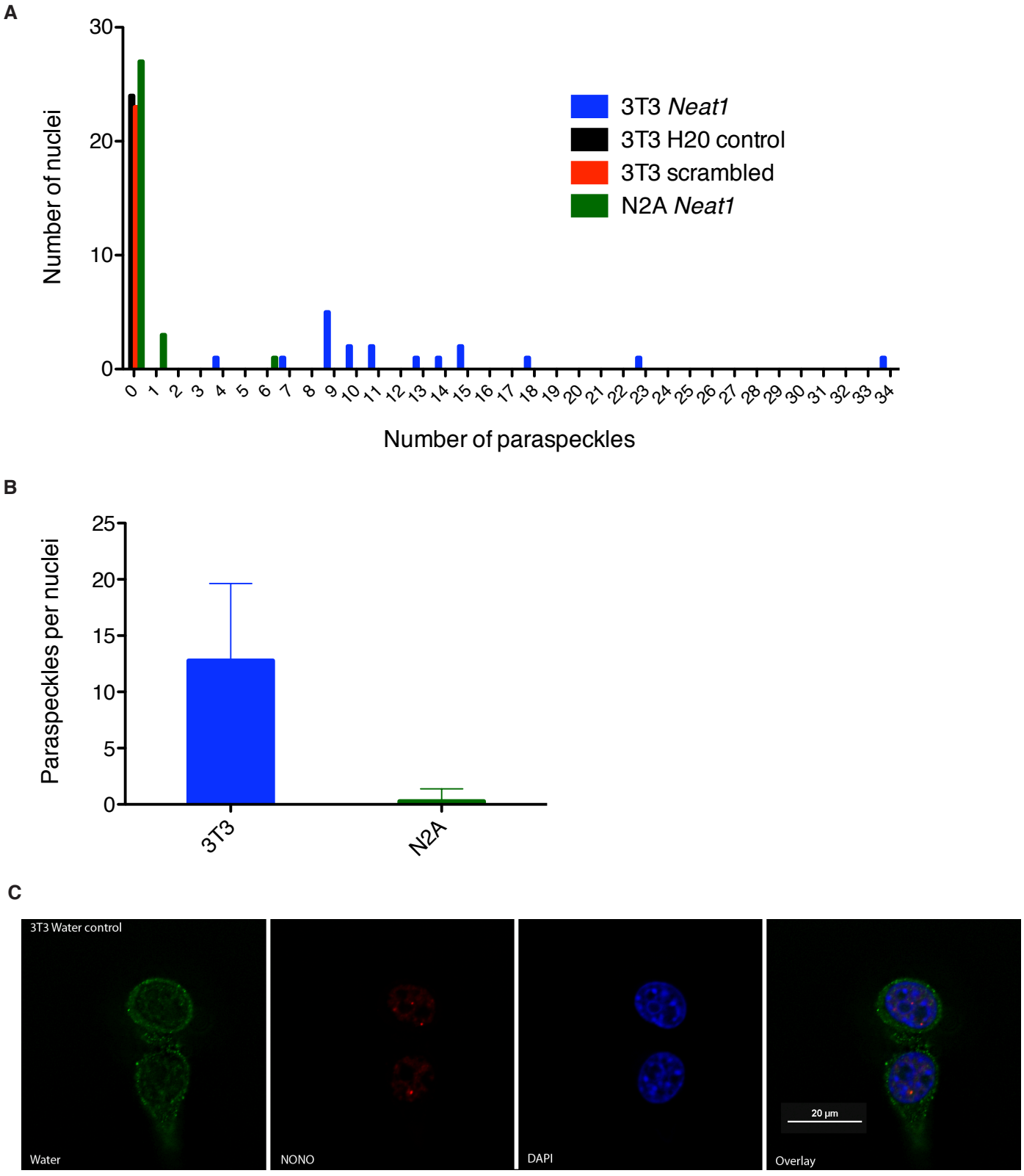

Figure S12: Paraspeckle quantification
A) Number of paraspeckles observed per nuclei from 3T3 and N2A *Neat1* FISH plus control FISH were counted (see methods). Graph shows distribution of paraspeckle numbers. B) Average number of paraspeckles per nuclei from counting in (A). Error bars show standard deviation. C) Control FISH on 3T3 cells. H20 used instead of *Neat1* probe. No paraspeckles were detected in H20 only 488 channel. TRITC labeled NONO protein (red) still detects paraspeckles as expected.

Supplementary Figure 13

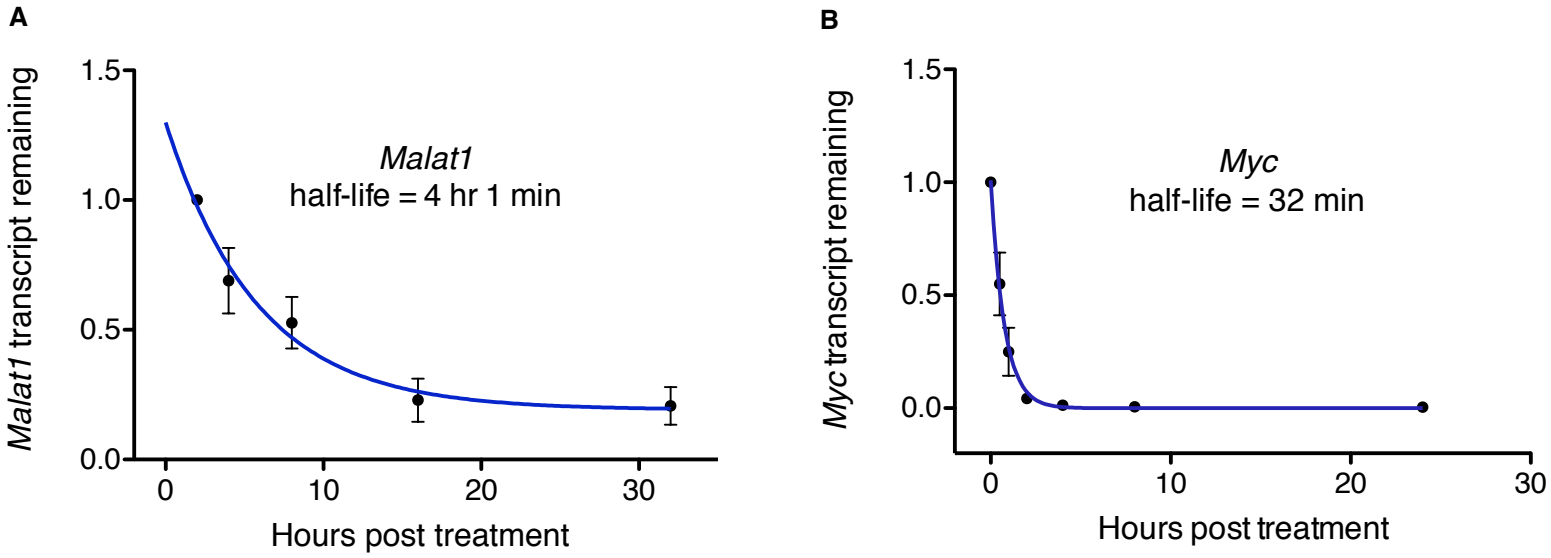

Figure S13: Transcript decay curves
Transcript decay curve for *Myc* in 3T3 cells after blocking transcription with Actinomycin D and measuring transcript remaining relative to *Gapdh* by qPCR. Fit modeled by one phase decay using nonlinear least squares regression. Error bars are standard deviations. 3 biological replicates. A) *Malat1* decay rate in N2A cells. Half-life 4 h 1 min (95% CI = 2 h 42 m to 7 h 48 min). *Malat1* produced unusual array results including increased expression levels after transcriptional blocking. This effect was also observed by qPCR in several samples whereby expression appears to increase for 2 h after transcriptional blocking before decreasing. Past approaches have also noted this issue in a small number of genes (Narsai et al. 2007) and determined the half-life by calculating decay from the latter time point with the highest expression, this same procedure was applied here. B) *Myc* decay rate in 3T3 cells. Half-life 32 min (95% CI = 27 - 39 min).

Narsai R, Howell KA, Millar AH, O'Toole N, Small I, Whelan J. 2007. Genome-wide analysis of mRNA decay rates and their determinants in Arabidopsis thaliana. *Plant Cell* **19**: 3418-3436!